Supporting information

Robust and flexible bulk superhydrophobic material from silicone rubber/silica gel prepared by thiol-ene photopolymerization

Yongsheng Li[a, b], Meng Ren[b], Pengfei Lv[b], Yinzhi Liu[b], Hong Shao[b], Cong Wang[b], Changyu Tang[b*], Yuanlin Zhou[c], Maobing Shuai[a*]

a. Science and Technology on Surface Physics and Chemistry Laboratory, Mianyang, 621907, China.

b. Chengdu Green Energy and Green Manufacturing Technology R&D Center, Chengdu Development Center of Science and Technology, China Academy of Engineering Physics, Chengdu, 610200, China.

c. State Key Laboratory for Environment-friendly Energy Materials, Southwest University of Science and Technology, Mianyang, 621000, China.

* Address correspondence to:

Changyu Tang: sugarchangyu@163.com;

Maobing Shuai: shuaimaobing@caep.cn

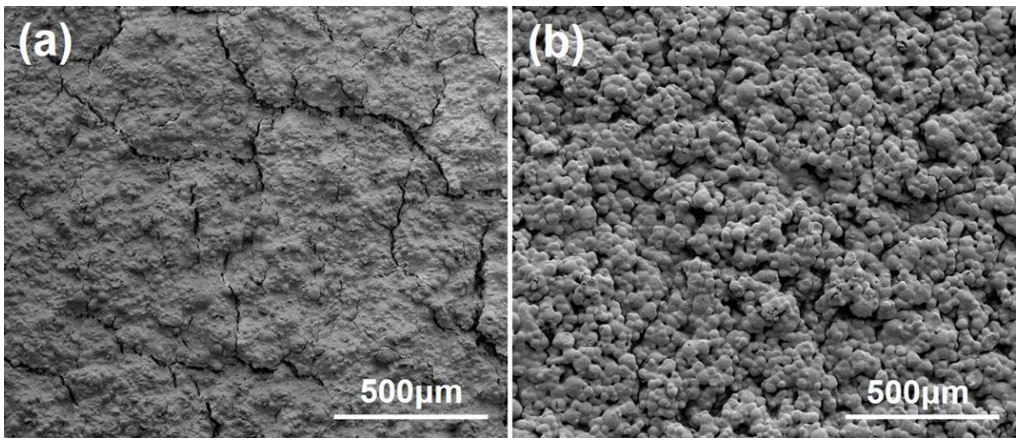

Fig. S1 SEM images of surface morphology for the composite coatings fabricated with two different micro-silica particles: (a) 3–5 μm and (b) 10–20 μm when their nano-silica/micro-silica ratios (3:5) are the same.

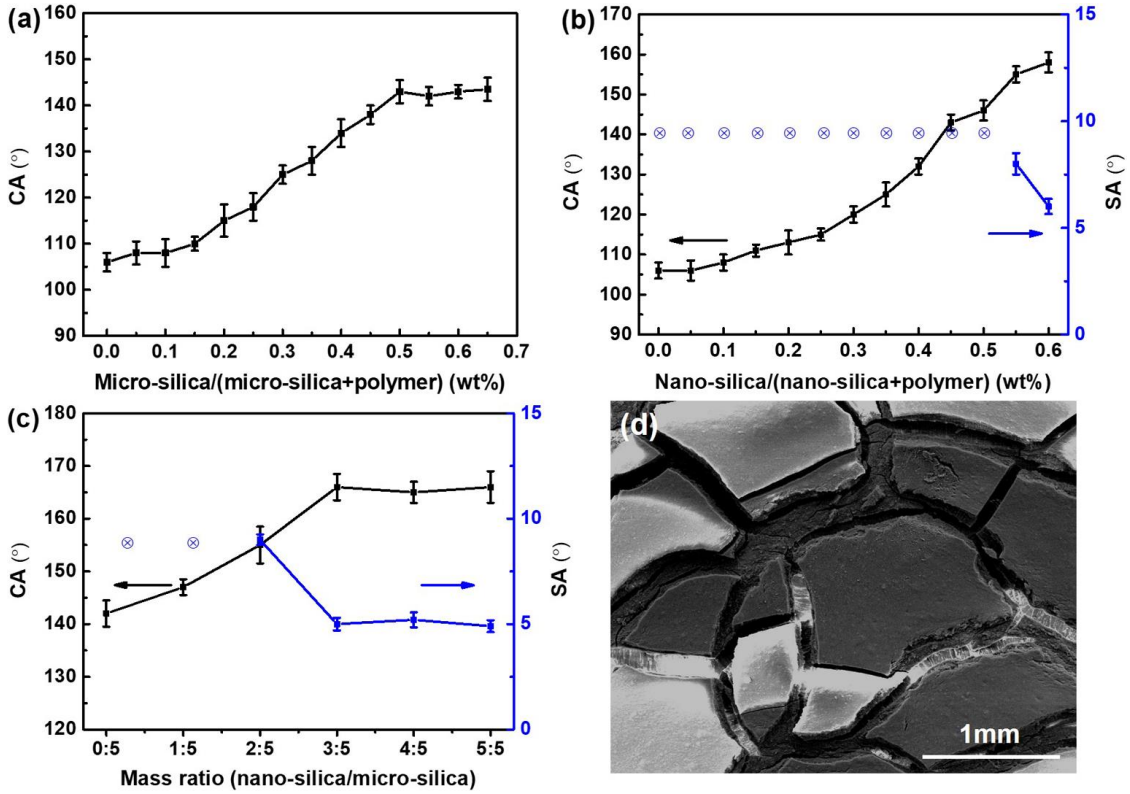

Fig. S2 (a) CAs and SAs of composite films with various mass fraction of (a) micro-silica and (b) nano-silica. (c) CAs and SAs of composite films with various

mass ratios of nano-silica and micro-silica. (d) SEM images of surface morphology for mass fraction 45% of (b). ⊗ indicates that water droplet cannot slide on the film.

Both nano-silica and micro-silica were used to create micro-nano roughness for superhydrophobic surface. The contents of micro-silica and nano-silica particles have great influence on the wetting of the composite coating. Thus, the micro-silica/nano-silica and silica/polymer ratios in composite coating were optimized and the related data were shown in Figure S2. With increasing micro-silica content alone, the contact angle (CA) of the composite increases and reaches a saturated value (~142°) at a mass ratio over 50% (Fig. S2a). This result indicates that the superhydrophobic film cannot form with addition of micro-silica alone. With addition of nano-silica (over 55%), the superhydrophobic film can be obtained (Fig. S2b). However, a large number of cracks are formed in the film at nano-silica content of 45% and lead to poor mechanical strength of the film due to nanofiller aggregate (Fig. S2d). Therefore, micro-silica and nano-silica is combined together to fabricate superhydrophobic film with good mechanical strength. The composite film can exhibit Cassie superhydrophobicity (CA ≈ 160° and SA ≈ 5°) when mass ratio of nano-silica and micro-silica is over 3:5 (Fig. S2c). In this case, the film is flexible and stretchable. Accordingly, the mass ratio of the polymer matrix and silica particles is 5:8.

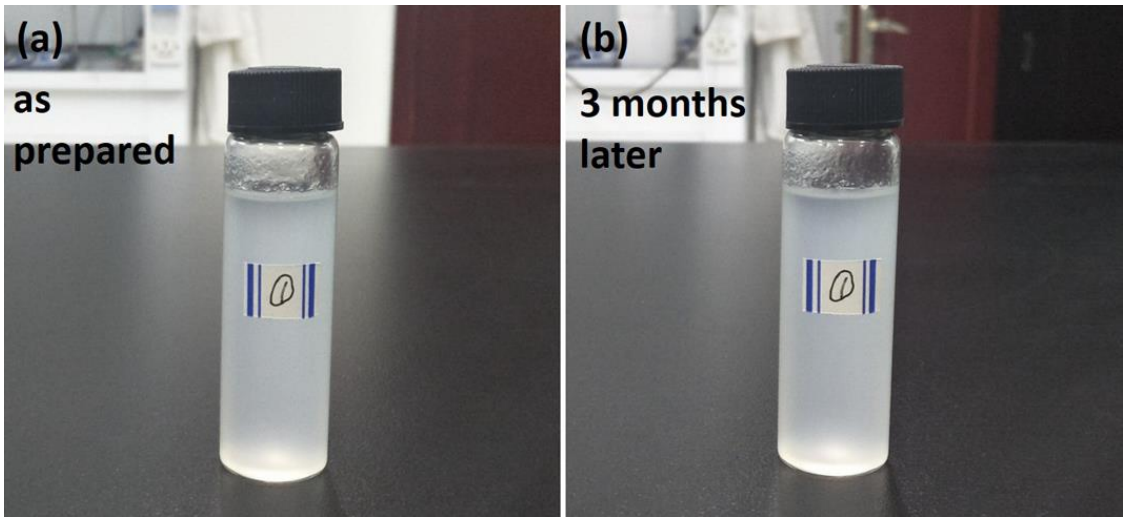

Fig. S3 Photographs of suspension of PDMS/silica/cyclohexane storage for different time at room temperature.

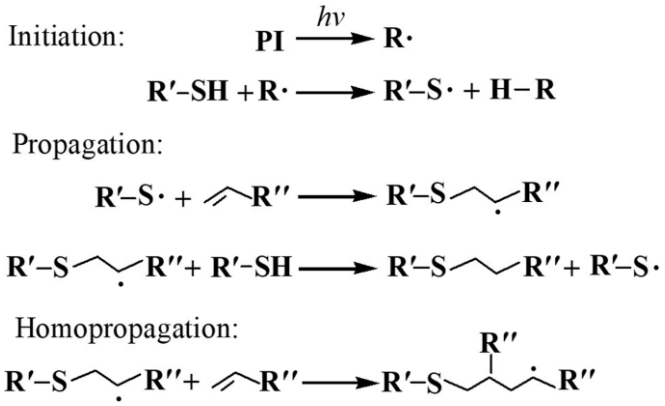

Fig. S4 Mechanism of thiol-ene addition reaction triggered by UV light.

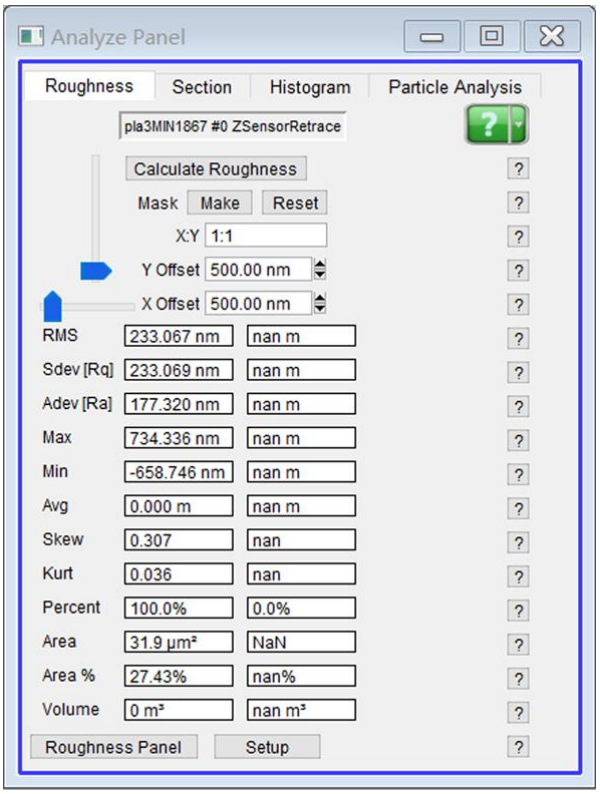

Fig. S5 Root mean-square (RMS) roughness of mico-mastoid obtained by AFM test.

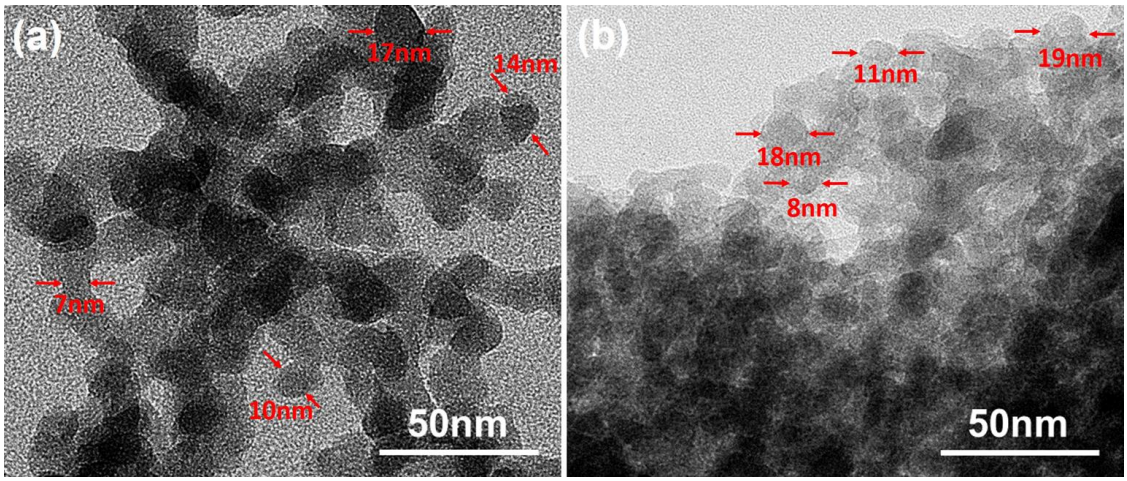

Fig. S6 TEM images of (a) original nanoparticles and (b) nano-silica in the mastoids.

Transmission electron microscopy (TEM) observation. The distribution of nano-silica on the mastoid surface was observed by TEM (Libra 200FE, Zeiss, Germany) at an acceleration voltage of 200 kV.

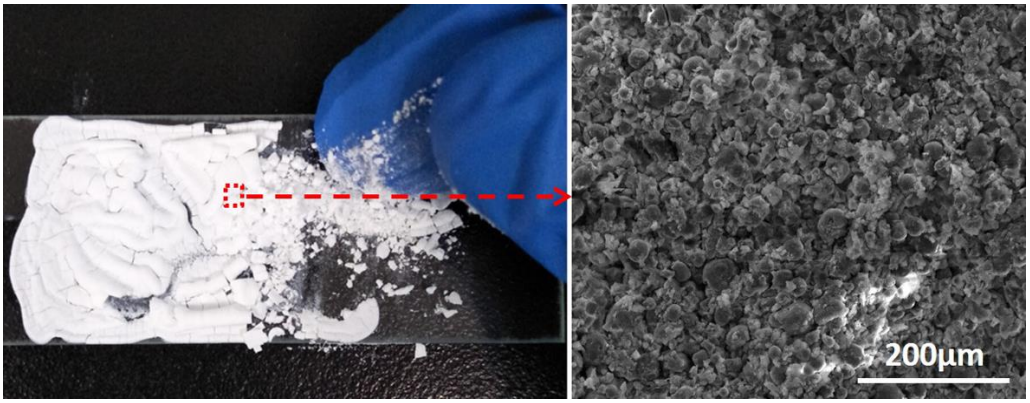

Fig. S7 Photograph and SEM image of UV cured PDMS/silica film prepared without cyclohexane. PDMS cannot binder silica together to form a free-standing film.

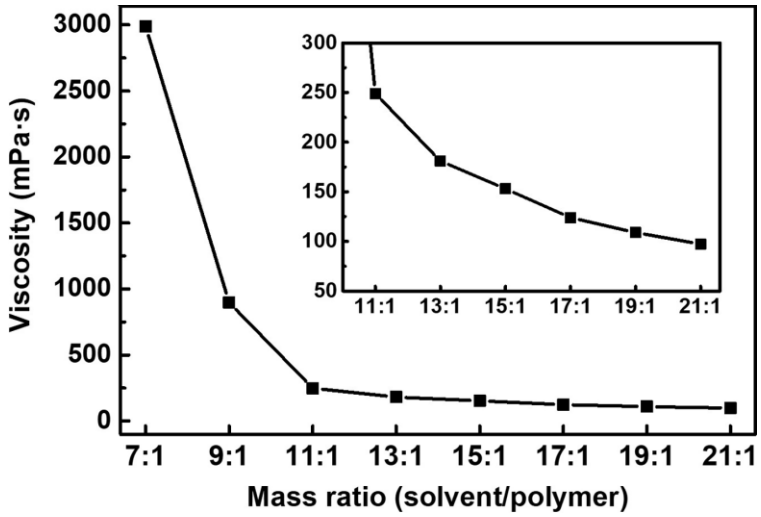

Fig. S8 Viscosities of suspensions with various mass ratios of solvent and polymer.

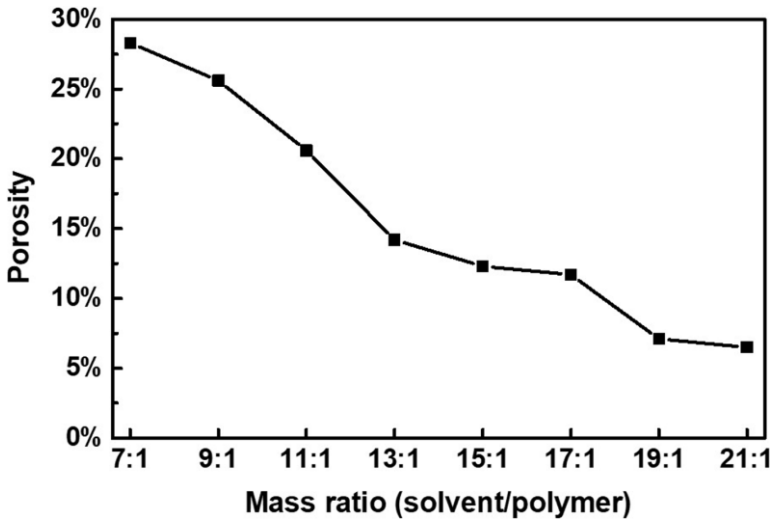

Fig. S9 Porosity of superhydrophobic film with various mass ratios of solvent and polymer.

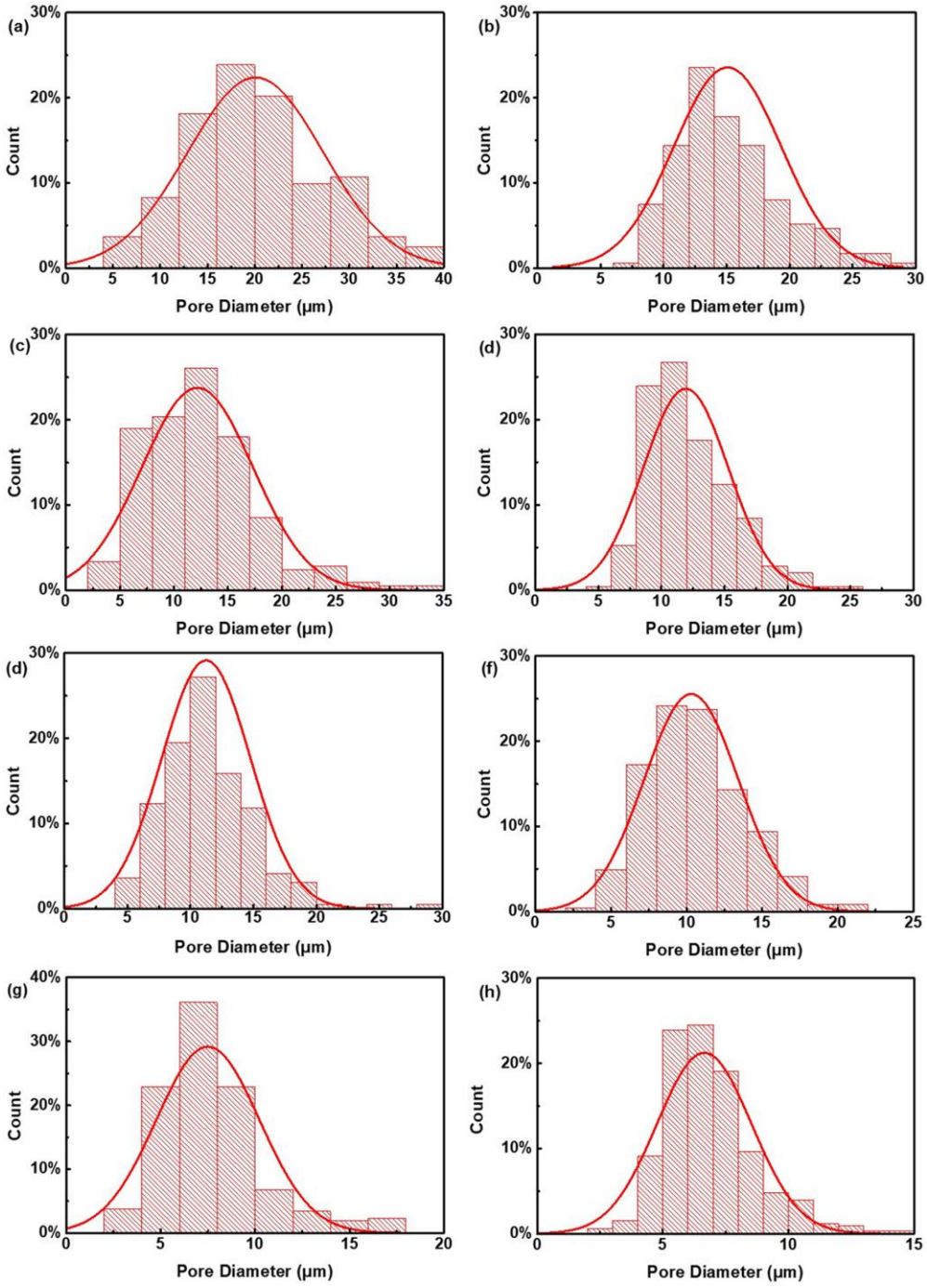

Fig. S10 Histograms showing the pore sizes of superhydrophobic films with various mass ratios of solvent and polymer: (a)7:1, (b)9:1, (c)11:1, (d)13:1, (e)15:1, (f) 17:1, (g)19:1, and (h) 21:1.

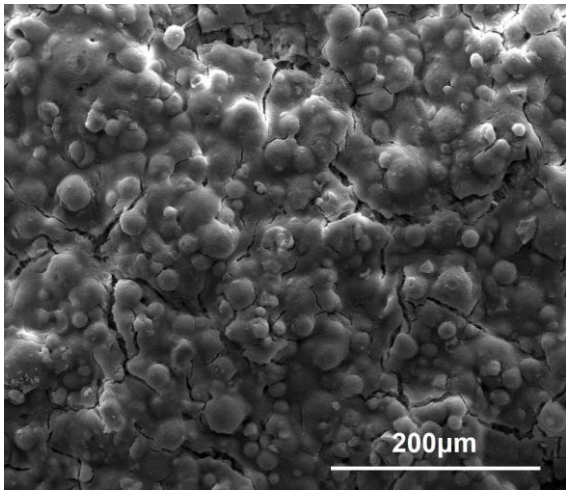

Fig. S11 SEM image of surface morphologies from superhydrophobic film after 1000-cycle stretching-releasing.

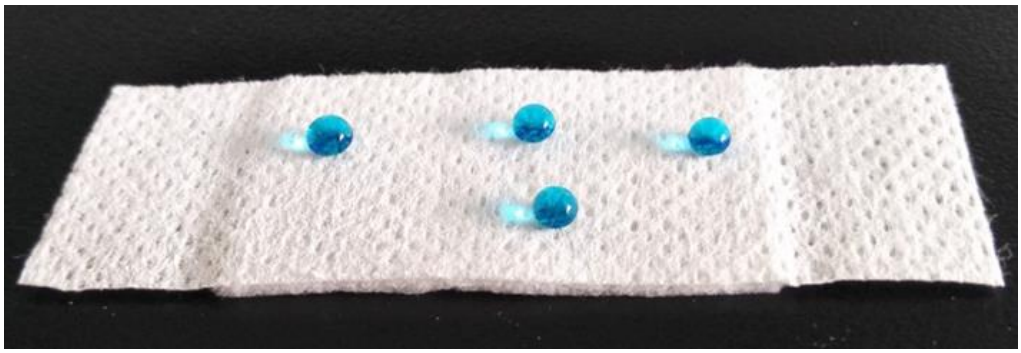

Fig. S12 The superhydrophobic dressing after 100 cycles of sandpaper abrasion.

Table S1. Water vapor permeability of pristine and coated dressing.

Sample	Water vapor permeability （$g/m^2 \cdot 24h$）
Pristine wound dressing	3050±31
Coated wound dressing	2389±27